Microstrip Low-pass Filter with Sharp Roll off and Wide Stop-band Using Multiple Cascaded Modified Radial Stubs Resonators

Hamid Radmanesh[1], A. Zhaleh[2]
[1]*Electrical Engineering Department,Shahid Sattari Aeronautical University of Science and Technology, Tehran, Iran*
[2]*Department of Electrical Engineering, Ashtian Branch, Islamic Azad University, Ashtian, Iran*
Hamid.radmanesh@aut.ac.ir, Ashkan_zhaleh@yahoo.com
Corresponding author: Dr. Hamid Radmanesh

***Abstract*- This paper presents a novel microstrip low-pass filter with good performance. A complete detailed theoretical analysis for the proposed filter is given using equivalent circuit models. The proposed filter applying multiple cascaded modified radial stubs resonators provides a sharp cut off frequency response that has a 185 dB/GHz roll off rate. Also, U-shaped attenuators provide a wide stop-band about $14f_c$ with more than -20 dB rejection. The filter has an insertion loss less than 0.027 dB from dc to 1.31 GHz. The experimental results are in fair agreement with the simulated results.**

***Index Terms*-** Low-pass filter, Microstrip, Radial stub, Sharp roll, Wide stop-band.

A. INTRODUCTION

Nowadays, the pass of *VHF*, *HF*, *L* bands and the suppression of spurious signals are the most requirements in marine, cordless and military communications. Microstrip low-pass filters with a low insertion loss, wide stop-band, sharp roll off and compact size are used to achieve these goals. Several techniques for the LPF design have been reported. The DGS filters have some problems in manufacturing applications such as radiation fields from defected structures and requiring a specific box [1]. These structures usually have high insertion loss and low return loss in their pass band [2-3]. Planar filters that are implemented using printed circuit technologies are generally preferable because of their easy fabrication and low cost as well as easy integration with other microwave circuits [4]. In [5], a LPF using open stubs loaded spiral has been presented, which has low radiation and scattering effects due to thinned out substrate, also it has low insertion loss and high return loss and it is compact size, but it has a gradual transition band. In [6], a LPF with a dual transmission line has been

Manuscript received 18-May-2016 and revised 6-Sept.-2016, *P- ISSN: 2322-4088*
Accepted on 12- Nov.-2016 *E- ISSN: 2322-3936*

presented, which has a sharp roll off, but it is not compact and has a narrow stop-band. In [7], a LPF

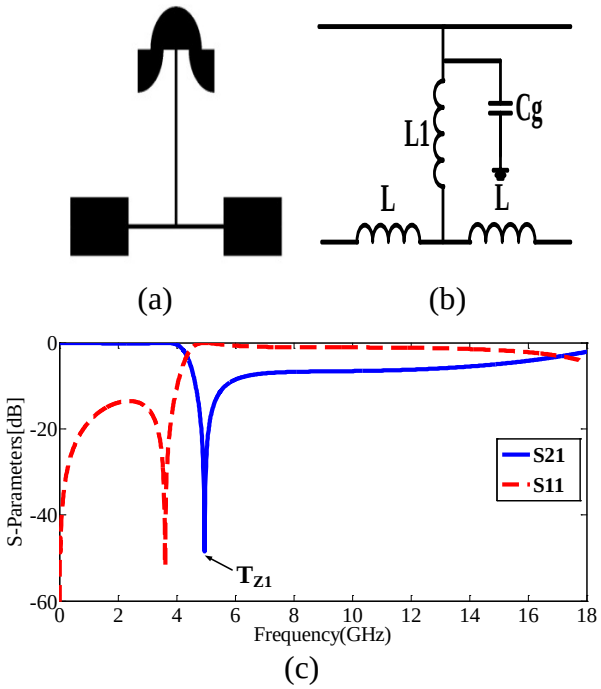

Fig. 1. One modified radial stub. (a) Layout. (b) LC equivalent circuit. (c) Simulated frequency Response of the proposed LPF.

with modified hairpin units has been presented, which has a high roll off rate and return loss is desired, but the filter is not compact size. In [8], a tunable LPF with stepped impedance hairpin resonator has been presented, which was controlled by different applied voltages. This filter has very sharp cut off frequency response with low insertion loss, but it does not have a wide stop-band. In many years ago, different realization of radial stub, are expressed with wide stop-band as an important specification [9-13]. The disadvantages of these structures are the graduate frequency response, a low return loss in the pass-band region and their complex topologies.

In this paper, a novel low-pass configuration using multiple cascaded modified radial stubs (MRSs) is designed, fabricated and tested. The lumped equivalent circuits are presented and adjusted. The proposed LPF the advantage of a wide stop-band up to $14f_c$ with seven attenuation poles in the stop-band. The proposed LPF provides excellent skirt selectivity, high sharp roll off and desired insertion loss and return loss.

II. FILTER DESIGN

Fig. 1 (a) shows the basic layout of a high impedance line connected with modified radial stub (MRS), whereas the layout is modeled by an LC equivalent circuit in Fig. 1 (b). The parameters of *L* and *C* are obtained as follows [14]:

$$L=\frac{Z\sin(\beta l)}{\omega}, \qquad (1)$$

$$C=\frac{1-\cos(\beta l)}{\omega Z \sin(\beta l)}, \quad (2)$$

Table I. LC values of the proposed filter.

Elements	**L**	**L1**	**Cg**
Values	1.26 nH	2.78 nH	0.37 pF

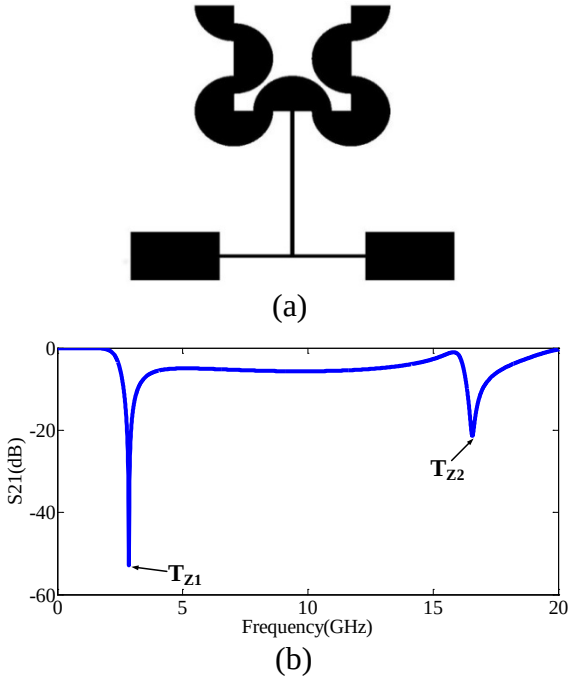

Fig. 2. Modified radial stubs with the addition of inductance. (a) Layout. (b) Simulated S21 parameter.

where, ω is the angular frequency, β is the phase constant, l is layout length and Z=50 ohm. Table I shows the values of *L* and *C*. Fig.1 (c) shows the frequency response of the resonator, with -3 dB cut off frequency (f_c) of 4.34 GHz and one transmission zero i.e. T_{Z1} at 4.95 GHz with -48.46 dB attenuation level. The value of the cut off frequency is not desired in this design. To acheive a method for designing the resonator, transfer function is adopted, because frequency responses of the resonator is formed based on poles and zeros. Equations of poles and zeros can be calculated by transfer function. The transfer function is penned in Eq. 3. *r* is matching resistance (*r* = 50 Ω)

$$\frac{vo}{vi}=\frac{r(1+CgL1s^2)}{(50+Ls)(2+Cgrs+CgLs^2+2CgL1s^2)} \quad (3)$$

As shown in Fig. 2 (a), by adding new MRS to the resonator, because of creating coupling capacitor between MRS and ground, a new transmission zero i.e. T_{Z2} will be generated, also i.e. T_{Z1} moves to 2.85 GHz point, which leads to reduce cut off frequency (f_c) to 2.39 GHz point, to have sharper roll off, as shown in Fig. 2(b).

According to the Fig. 3 (a), the other coupling capacitor can be added to the resonator, which

causes to have new other transmission zeros i.e. T_{Z3} and i.e. T_{Z4} at 23.58 GHz and 26.89 GHz with

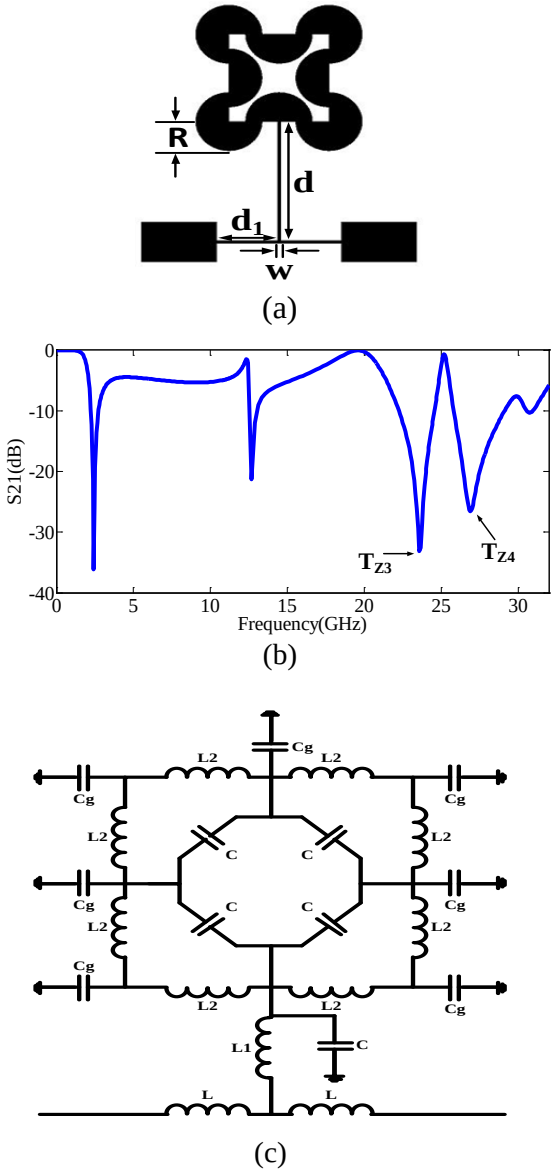

Fig. 3. Modified radial stubs resonator. (a) Layout. (b) Simulated S21 parameter. (c) LC equivalent circuit.

according attenuation levels of -33.13 dB and -26.55 dB, respectively. Also transmission zeros of T_{Z1} and T_{Z2} are reduced, which leads to reduce cut off frequency (f_c) to 1.97 GHz point, as illustrated in Fig. 3 (b). An equivalent circuit model of the proposed LPF is presented in Fig. 3 (c). In this circuit model that has symmetrical structure, L is the equivalent inductance of feeding line with length of d_1 and width of W; L_1 is related to the line with length of d and width of W; L_2 is the inductance of modified radial stubs with radial of R; C is the coupled capacitance between two modified radial stubs; C_f is the resultant capacitance modified radial stub and the feeding line; C_g is capacitance of modified radial stubs with respect to ground. Table II gives the LC elements values of the proposed equivalent circuit, which are synthesized and optimized based on the elliptic function response by using Agilent Advanced Design System (ADS) as a tuning tool. Fig. 4, shows the simulation results of

the proposed layout and *LC* model, which are almost overlapped.

Table II. LC values of the filter using one MRS resonator.

Elements	**L**	**L1**	**L2**	**C_g**	**C_f**	**C**
Values	0.88 nH	1.84 nH	50 fH	0.29 pF	0.25 pF	0.01 pF

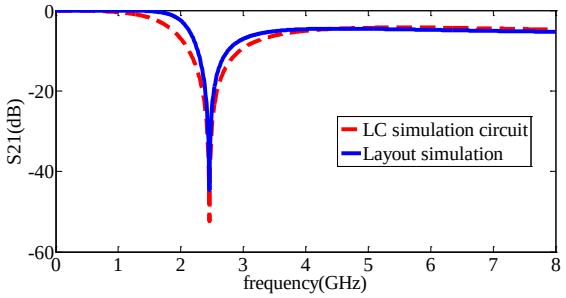

Fig. 4. Simulated S21 parameter L-C and layout

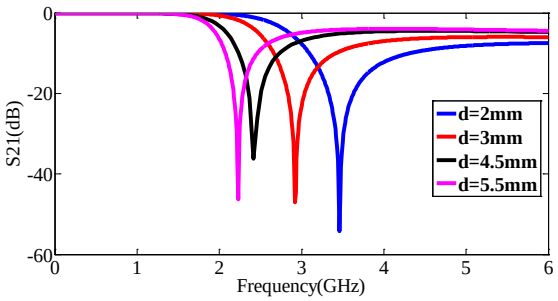

Fig. 5. Comparison of the simulated S21 parameter with different d lengths

As seen from Fig. 5, by increasing length of *d* from 2 mm to 5.5 mm, because of decreasing the inductance of L_1, the transmission zero moves to the a lower frequency from 3.46 GHz to 2.23 GHz with better sharp roll off.

As shown in Fig. 6, by decreasing width of *W* from 0.5 mm to 0.1 mm, the capacitance of C_f decreases and the transmission zero moves to the lower frequency from 3.19 GHz to 2.42 GHz. As shown in Fig. 7, by increasing radius of *R* from 0.8 mm to 2 mm, the inductance of L_2 increases and transmission zero has a perceptible variation from 3.24 GHz to 1.44 GHz.

Due to the evident changes, the length of *d* and the width of *W*, plays an important role in improving the roll off performance. As mentioned and using ADS software as a tuning tool, the best range roll off performance considering the size of the proposed resonator is obtained as *d* when, is 4.5 mm and *W* is 0.1 mm. The location of cut off frequency will be controlled by radial *R*. Good cut off frequency value according to desired performance, is selected when *R* is 1.1 mm.

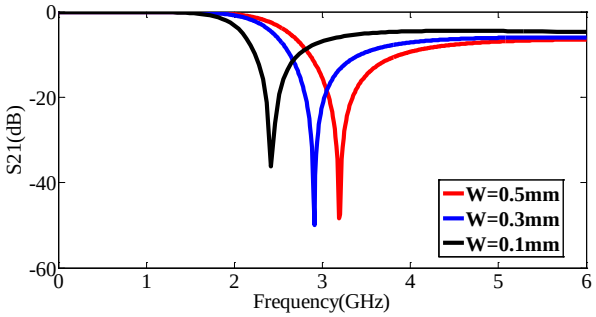

Fig. 6. Comparison of the simulated S21 parameter with different *W* width

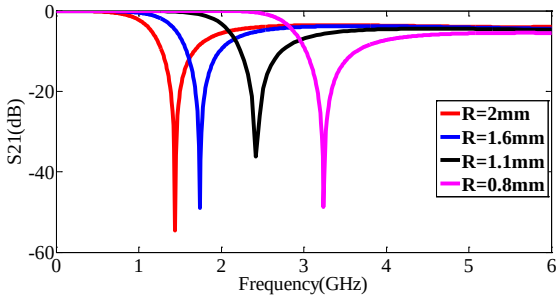

Fig. 7. Comparison of the simulated S21 parameter with different *R* radial

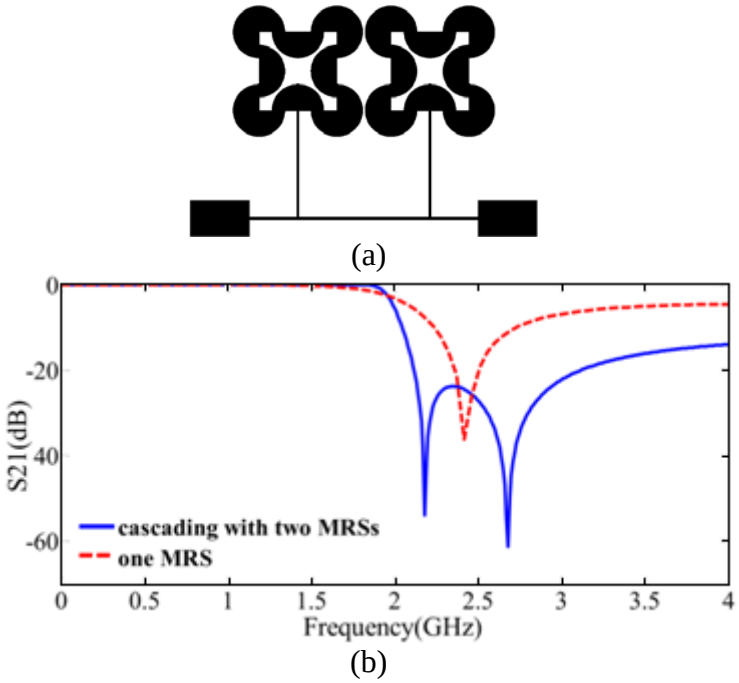

Fig. 8. Modified radial stubs resonator by cascading. (a) Layout. (b) S21 parameters of proposed resonator with one MRS and two MRSs.

To have an even broader stop-band and a better roll off, two MRSs resonators are cascaded as shown in Fig. 8 (a). The two cells are connected by a short inductance with a narrow width. As illustrated in Fig. 8 (b), when we have one MRS, transition band is 0.37 GHz from -3 dB to -20 dB, but by cascading two cells together, new transmission zero was obtained at 2.18 GHz with -53.92 dB attenuation level, which causes to have a sharper roll off. In this case, the transition band is 0.15 GHz from -3 dB and -20 dB.

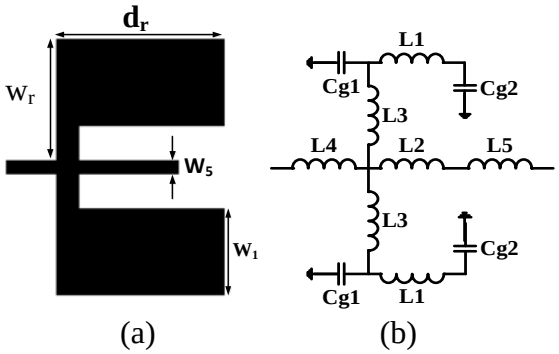

Fig. 9. U-shaped attenuator. (a) Layout. (b) LC equivalent circuit.

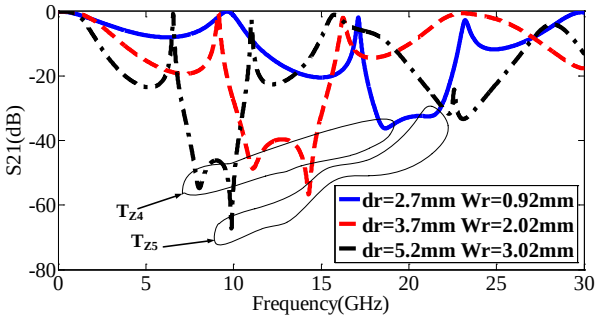

Fig. 10. Simulated S21 parameter of an U-shaped attenuator with different d_r and W_r.

To increase the stop-band band width (SBW), U-shaped attenuator is recommended in Fig. 9 (a). Fig. 9 (b) shows *LC* equivalent circuit of the proposed attenuator, which L_4 and L_5 are the inductances introduced with width of W_5. L_3 is the inductance introduced with length of W_r. L_1 is the inductance introduced by d_r and L_2 is inductance of the ended rectangles introduced by W_r. C_{g1} and C_{g2} are the capacitances of different parts of the filter with respect to ground. Equation (3) shows that the U-shaped attenuator depends on L_1 and Z_{tot} where each one depends on length of d_r and width of W_r[15]. As shown in Fig. 10, transmission zeros of T_{Z4} and T_{Z5} are moved by changing the size of d_r and W_r. As can be seen, these changes cannot increase stop bandwidth enough, lonely. As shown in Fig. 11 (a), we can add another U-shaped attenuator with different d_r and created coupling capacitors of C_1 and C_2 between U-shaped attenuators which causes to generate new transmission zeros and increase stop-band bandwidth.

$$\begin{pmatrix} A & B \\ C & D \end{pmatrix} = \begin{pmatrix} Z_{tot} & det[Z] \\ 0 & Z_{tot} \end{pmatrix} \begin{pmatrix} -1 \\ L_1' S \end{pmatrix}, \tag{4}$$

Where: $L_1' = \frac{L_1}{2}$; $det[Z] = \left(\left[(L_1' + L_3)S + S^{-1}\left(\frac{1}{Cg1}\right)\right]\right)^2 - (L_1' S)^2)$; $Z_{tot} = (L_1' + L_3)S + S^{-1}\left(\frac{1}{Cg1}\right)$.

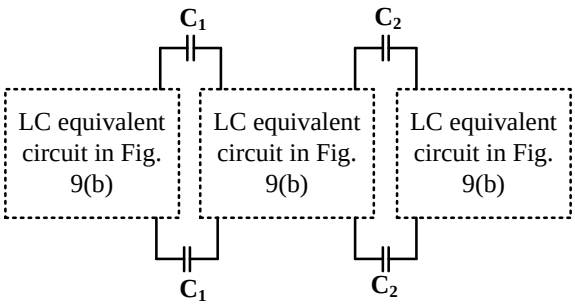

Fig. 11. LC equivalent circuit by considering coupling capacitors.

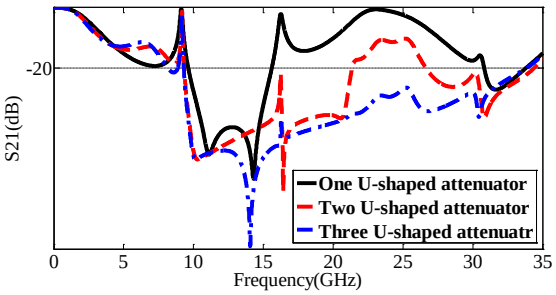

Fig. 12. Simulated frequency responses S21 for one, two and three U-shaped attenuator

As seen from Fig. 11 (b), the one U-shaped attenuator creates two transmission zeros at 11.11 GHz and 14.29 GHz that makes a high attenuations in higher frequencies from 9.62 GHz to 15.60 GHz, which make stop bandwidth (SBW) about 5.98 GHz. To increase more stop-band bandwidth, another U-shaped attenuators has been used that creates coupling capacitor and the stop bandwidth can change from 9.33 GHz to 21.36 GHz, which has been 2SBW. With the addition of third U-shaped attenuators, transmission zeros move to 14.06 GHz and 30.44 GHz with attenuation level -79.04 dB and -36.24 dB, respectively. It provides better wide rejection band from 9.30 GHz to 33.87GHz, which is about four times of the initial value (4SBW).

III. Fabrication and Measurement

In order to understand the characteristics of the proposed filter, a prototype LPF with f_c of 1.97 GHz is fabricated on the RT/Duorid 5880 substrate (h = 0.508 mm, ε_r = 2.2 and tanδ = 0.0009). Fig. 13 (a) depicts the microstrip layout of the proposed LPF. The optimized dimensions of the filter are $w = 0.1$ mm, $w_1 = 1.9$ mm, $w_2 = 1.55$ mm, $w_3 = 2$ mm, $w_5 = 0.3$ mm, $d = 4.5$ mm, $d_1 = 2$ mm, $d_2 = 9.7$ mm, $d_r = 3.7$ mm, $d_{r1} = 2$ mm, $d_{r2} = 0.9$ mm, $d_{r3} = 1$ mm, $d_{r5} = 0.5$ mm, $d_{r6} = 0.7$ mm, $R = 1.1$ mm. The size of the filter is 21.3 mm × 11.75 mm ($0.191\,\lambda_g \times 0.105\,\lambda_g$, where λ_g is the guided wavelength at f_c). Fig. 13 (b) illustrates the photograph of the proposed LPF. All of the simulations are performed using EM simulator (ADS) and the measurement are done using the HP8757A network analyzer. Fig. 13 (c) shows measured and simulated S-Parameters of the proposed microstrip LPF, that it is predominately attributed to the MRS size and suppression level

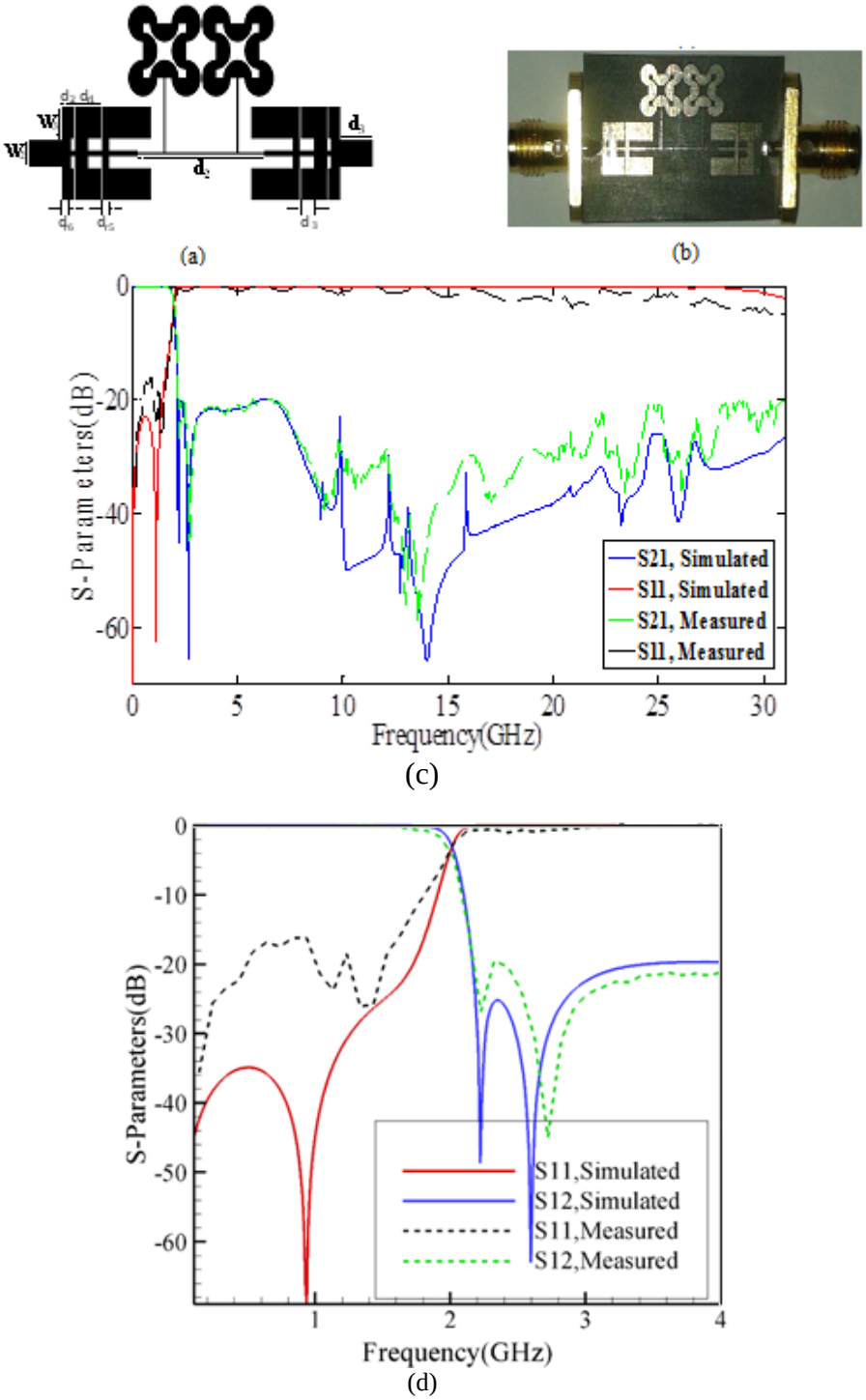

Fig.13. (a) Layout. (b) Fabricated MRSs LPF (c) simulated and measured S-parameters of the proposed filter (d) simulated and measured S-parameters of the proposed filter at the pass band

better than -20db from 2.13 GHz up to 31 GHz that show we reach a wide stop-band with high attenuator level. The transition band is 0.2 GHz from -3 dB to -40 dB. A low insertion loss less than

Table III. comparison between the proposed LPF with published LPFs

Ref	f_c	R_L	I_L	ζ	RSB	NCS	FOM
[4]	1.18	40	-	36	1.32	0.079×0.079	11543
[6]	1.04	18	0.5	135	0.44	0.18×0.22	5181
[11]	3.2	18	1	5.9	1.66	0.12×0.063	2586
[12]	1.76	14	0.4	95	1.6	0.104×0.123	27292
[16]	0.5	16	0.5	95	1.58	0.104×0.214	13488
This work	**1.97**	**23**	**0.03**	**185**	**1.76**	**0.191×0.105**	**32317**

0.027 dB in the pass-band from DC to 1.31 GHz. These plots reveal good resemblance between simulated and measured results. Moreover, performance comparison with related works in the literature is summarized in Table III. In this table:

The roll-off rate is defined as:

$$\zeta = \frac{a_{\max} - a_{\min}}{f_s - f_c} \tag{5}$$

where, a_{max} is the 40 dB attenuation point $a_{\min}$ is 3dB attenuation point, f_s is the 40dB stopband frequency, f_c is the 3dB cutoff frequency. The relative stop-band bandwidth (RSB) is given by:

$$\text{RSB} = \frac{\text{stopband bandwidth}}{\text{stopband centre frequency}} \tag{6}$$

The normalized circuit size (NCS) is formulated as:

$$\text{NCS} = \frac{\text{physical size (length} \times \text{width)}}{\lambda g^2} \tag{7}$$

This is applied to measure the degree of miniaturization of diverse filters, where λ_g is the guided wavelength at 3 dB cutoff frequency. Finally, the figure-of-merit (FOM) is the overall index of a proposed filter, which is defined as:

$$\text{FOM} = \frac{\zeta \times \text{RSB} \times \text{SF}}{\text{NCS} \times \text{AF}} \tag{8}$$

The suppression factor (SF) is equal 2, because stop-band bandwidth is calculated under 20 dB limitation. The architecture factor (AF) is equal 1, because the design is 2D.

Table III compares the proposed LPF with published LPFs. The size of proposed LPF is more compact from [6],[16] and [17]. The proposed LPF has the best insertion loss, also has return loss

better than the other LPFs except [4]. The proposed LPF has the highest roll-off rate (185 dB/GHz) among the reported filters, of course in [6] $a_{\max}$ was considered in 20dB in equation (5). The proposed LPF has the most desirable relative stop-band bandwidth, even it is better than [4] considered SF considered of 1.5. However, SF was considered 2.3 in equation (8), in [12]. Finally the proposed LPF has figure of merit much greater than other the reported filters.

IV. CONCLUSION

The design of a microstrip low pass filter is presented using modified radial stubs resonator with 185dB/GHz roll off rate. One of the main features of the proposed cell is the creation of transmission zeros without increasing the size in comparison of conventional resonators. By using U-shaped attenuators the stop-band width equal to $14f_c$ can be achieved. The insertion loss is better than 0.027 dB and return loss is better than 23 dB in the pass-band region. Results indicate that the demonstrators achieve a high figure-of-merit of 32317. With these features, this kind of LPF will be useful in modern communication systems.

REFERENCES

[1] M. N. Jahromi, "Wide stopband compact microstrip lowpass filter using circular ring resonator and split ring resonators," Microwave and Optical Technology Letters, vol. 53, no. 9, pp. 1961-1964, Sep. 2011.

[2] A. Faraghi, M. N. Azarmanesh, M. Ojaroudi, "Small Microstrip Low-Pass Filter by using Novel Defected Ground Structure for UWB Applications," Appl. Comp. Electro Society (ACES) Journal, vol. 28, no. 4, pp. 341-347, April 2013.

[3] H. Taher, "High-performance low-pass filter using complementary square split ring resonators defected ground structure," IET Microwaves, Antennas & Propagation, vol. 5, lss. 7, pp 771-775, 2011.

[4] J. Wang, L.-J. Xu, S. Zhao, Y.-X. Guo and W. Wu, "Compact quasi-elliptic microstrip lowpass filter with wide stopband," Electronics Letters, vol. 46, no. 20, Sept. 2010.

[5] A. Adinehvand, A. Lotfl, "Compact Lowpass Filter with Wide Stop-Band using Open Stubs-Loaded Spiral Microstrip Resonant Cell," Appl. Comp. Electro Society (ACES) Journal, vol. 28, no. 1, 2013.

[6] V. K. Velidi, S. Sanyal, "Dual-Transmission-Line Microstrip Equiripple Lowpass Filter with Sharp Roll-Off," ETRI Journal, vol. 33, no. 6, pp. 985-988, 2011.

[7] M. Hayati, H. S. Vaziri, "Wide Stop-Band Microstrip Lowpass Filter with Sharp Roll-off Using Hairpin Resonators," Appl. Comp. Electro Society (ACES) Journal, vol. 28, no. 10, pp. 968-975, Oct. 2013.

[8] J. Ni, J. Hong, "Compact continuously tunable microstrip low-pass filter," IEEE Trans. on Microwave Theory Tech., vol. 61, no. 5, pp. 1793-1800, May 2013.

[9] M. Yang, J. Xu, Q. Zhao, L. Peng, G. Li, "Compact, broad-stopband lowpass filters using sirs-loaded circular hairpin resonators," Progress In Electromagnetics Research, 102, pp. 95-106. 2010.

[10] Y. Dou, J. Wang, H. Cui, J. L. Li, Miniaturized Microstrip Lowpass Filter with Ultra-Wide Stopband," Appl. Comp. Electro Society (ACES) Journal, vol. 28, no. 7, pp. 640-645. July 2013.

[11] K. Ma, K.S. Yeo and W. M. Lim, "Ultra-wide rejection band lowpass cell," Electronics letters, vol. 48, no. 2, 2012.

[12] M. Hayati, H. Asadbeigi and A. Sheikhi, “Microstrip lowpass filter with high and wide rejection band,” Electronics letters, vol. 48, no. 19, Sep. 2012.

[13] K. Ma, K. S. Yeo, “Novel low cost compact size planar low pass filters with deep skirt selectivity and wide stopband rejection,” In Microwave Symposium Digest (MTT), 2010 IEEE MTT-S International, pp. 233-236, May 2010.

[14] L. H. Hsieh, K. Chang, “Compact elliptic-function low-pass filters using microstrip stepped-impedance hairpin resonators,” IEEE Trans. on Microwave Theory Tech., vol. 51, no. 1, pp. 193-199. 2003.

[15] M. Hayati, F. Shama, “Compact microstrip low-pass filter with wide stopband using symmetrical U-shaped resonator,” IEICE Electronics Express, vol. 9, no.3, pp. 127-132, 2012

[16] V. K. Velidi, S. Sanyal, “Sharp roll-off lowpass filter with wide stopband using stub-loaded coupled-line hairpin unit,” IEEE Microwave and Wireless Components Letters, vol. 21, no 6, pp. 301-303. 2011.

[17] Seyyed Jamal Borhani, M. Amin Honarvar, and M. Reza Namazi Rad," A Compact UWB Bandpass Filter with High Selectivity and Dual Notched-Band” Journal of Communication Engineering, Vol. 4, No.2, pp.100-110, July-December 2015.